International Journal of Industrial Electronics, Control and Optimization © 2021 IECO
Vol. 4, No. 2, pp. 167-179, April (2021)

PWM Control Methods Based on Mathematical Equations for Z-Source Inverters

Taher Ahmadzadeh [1], Ebrahim Babaei [2, †], Mehran Sabahi [3], Taher Abedinzadeh [4]

[1, 4] Department of Electrical Engineering, Shabestar Branch, Islamic Azad University, Shabestar, Iran
[2, 3] Faculty of Electrical and Computer Engineering, University of Tabriz, Tabriz, Iran

ABSTRACT

In power converters, the total harmonic distortion (THD) can be decreased by using two strategies which are filtering and controlling methods. The filtering strategy is indeed costly because of using hardware devices (such as capacitors and inductors). A suitable strategy to control the modern power converters without using the hardware devices is the pulse width modulation (PWM) technique. In this paper, three new PWM control methods based on mathematical equations for various Z-source inverters (ZSIs) are proposed. Controlling the duty cycles of switches is the basic idea of these methods to control the output voltage. The proposed control methods are analyzed under the circumstances of constant input and balanced output voltage (CIBOV) and ripple input and balanced output voltage (RIBOV). The advantages of the proposed methods are control of voltage, current and harmonic distortion. Other advantages of these methods are lower value for THD and elimination of low-order harmonics. The correct operation of the proposed PWM techniques is proved by using the simulation results.

Article Info

Keywords:
Pulse width modulation (PWM), Quasi-Z-source inverter (qZSI), Shoot-through (ST) state, Total harmonic distortion (THD).

Article History:
Received 2020-06-01
Accepted 2020-10-14

I. INTRODUCTION

The dc-ac converters (or inverters) are suitable topologies for medium-power and high-power applications. Hence, these converters have a main role in the industry and urban lifestyle [1]-[4]. Up to now, various topologies of inverters have been presented such as inverters based on voltage source (VSIs), current source (CSIs), and impedance source (ZSIs). Each one of them has its own limitations that should be considered in switching states [4]-[8]. The inverter topologies based on the Z-source network have the capability of voltage boost by shoot-through (ST) states. Moreover, they are suitable for applications such as photovoltaic, fuel cell, motor drive, and wind turbine [7]-[10].

In a power converter, power losses can be lower by reducing the value of total harmonic distortion (THD). To achieve this aim, a suitable topology or control method can be employed. Moreover, filtering and controlling strategies can decrease the THD and eliminate low-order harmonics [1]-[3]. The filtering technique needs some hardware devices (such as capacitor and inductor). To decrease the size and cost of the filter, the higher switching frequency can be profitable which causes more switching losses. Hence, that's better to focus on control methods [1], [2], [11].

In the ac output of an inverter, the magnitude, frequency, and phase can be controlled by an appropriate control method. The pulse width modulation (PWM) techniques have the capability to control the switching states, and in comparison with other strategies can cause a decrease in low-order harmonics [1]-[3], [11]. UP to now, several PWM techniques for inverter based on Z-source topology have been introduced. The main purpose of them is a simple implementation, high voltage gain, low device stress, less commutation per switching cycle, and low harmonics and THD [12]-[18].

Three basic techniques are the simple boost control (SBC), maximum boost control (MBC), and maximum constant

†Corresponding Author: e-babaei@tabrizu.ac.ir
Tel: +98- 41-33393763, Fax: +98- 41-33300819, University of Tabriz
Faculty of Electrical and Computer Engineering, University of Tabriz, Tabriz, Iran

boost control (MCBC) [12]. In order to control the ST duty cycle (D_{sh}) in the SBC method, a triangular carrier wave is compared to two straight lines. But, in MBC and MCBC strategies, the ST states generate from the comparison of two envelope curves with the triangular carrier waveform. The ST time per switching cycle is constant for SBC and MCBC. But, it is variable for MCB. The MBC technique has a higher voltage boost factor and lower voltage stress across the devices in comparison with the two others. However, it has the drawbacks of low-frequency ripples on the Z-source network. In order to reduce the volume and cost of the LC network, the elimination of low-frequency current ripples is needed which is achieved by a constant ST duty cycle [12].

Other various solutions have been introduced in [13]-[15] to reduce the inductor current ripple for the ZSI topologies. In [13], a switching technique for the ZSI has been presented. This strategy has used the unequal ST time intervals to reduce the inductor current ripple. This method compared to the conventional method with equal ST time intervals can reduce the inductor current ripple by 27.8% without increasing the number of switching states. Also, to reduce this problem, [14] has employed the advanced bus clamping switching sequences as titled ABC4-MCB control method. This method in comparison with the ZSVM6-MCB strategy, for the equal average switching frequency, reduces the maximum instantaneous inductor current ripple around by 34%. In this technique, the reduction percentage of the inductor current ripple is constant over the entire range of the ST time interval (0-0.48). In [15], the current ripple of ZSI has been firstly analyzed. Moreover, a comparison between ZSI and VSI has been given in terms of current ripples. At last, a variable dc-link voltage and switching frequency method has been employed to reduce the conduction and switching losses without increasing the predicted peak current ripple.

Ref. [16] has introduced a dual switching frequency modulation algorithm for ZSI and qZSI to combine high-frequency PWM with low-frequency singular PWM which causes a reduction in the converter size as it operates at the high switching frequency.

In [17], several new control methods for single-phase ZSIs have been presented. Also, a comparison among them has been given. Moreover, an optimized closed-loop control scheme has been designed to eliminate more harmonic. These techniques in comparison with conventional boost control strategies have a simple algorithm, more flexible voltage gain, and lower harmonics.

In [18], an improved sinusoidal PWM (SPWM) method for the one-phase and multi-phases approaches of the quasi ZSIs (qZSIs) has been introduced. The main aim of this strategy is that a similar control signal at per time interval can be generated by the controller because one of the switches is turned on and the other one is turned off. Also, the switching state of another MOSFET can be produced by a NOT gate. In this paper, the related mathematical analysis of qZSI has been also provided and the controller is designed based on these calculations.

In [1] and [2], several PWM control methods for conventional VSI have been introduced. The basic idea of them is to control the duty cycles of the switches in such a way that a load sees a controllable average voltage. Inspired by [1] and [2], three new PWM control methods based on mathematical equations for various single-phase Z-source topologies have been proposed in this paper. Significantly, the proposed methods have been analyzed for a conventional single-phase qZSI. The main advantage of the proposed methods is based on the mathematical foundation. In other words, the proposed methods include some mathematical equations in which each one of them has a controllable capability. Other benefits of proposed methods are lower value for THD and elimination of low-order harmonics. This paper is categorized as follows. In section II, a brief review of the conventional single-phase qZSI topology is performed. In section III, the operating principle of three proposed PWM control methods with related equations is presented. Since the proposed methods can also generate the desired output voltage from a regulated and unregulated input voltage. So, in this section, these methods are analyzed under situations of CIBOV (constant input and balanced output voltage) and RIBOV (ripple input and balanced output voltage). Section IV provides a comparison between the proposed methods and other methods. The simulation results given in section V prove the correct operation of the proposed methods.

II. Conventional Quasi-Z-Source Inverter (QZSI)

Fig. 1 shows the conventional single-phase qZSI topology [19]. This inverter has two modes such as shoot-through (ST) and non-shoot-through (non-ST) switching states. The equivalent circuits of qZSI are shown in Fig. 2. Considering Fig. 2(a), in the ST switching state (T_{sh} time interval), the switches are turned on, whereas, the diode of D is turned off. In this mode, the following equations can be obtained:

$$v_{L1,sh} = V_{dc} + V_{C2} \quad , \quad v_{L2,sh} = V_{C1} \quad , \quad v_{o,sh} = 0 \qquad (1)$$

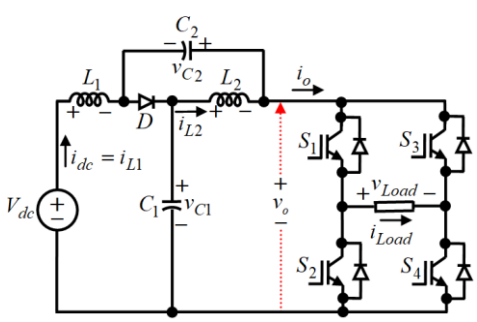

Fig. 1. Conventional single-phase qZSI topology [19].

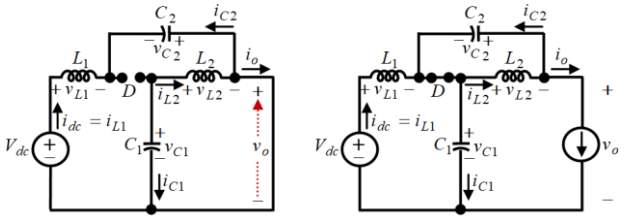

Fig. 2. Circuits of qZSI; (a) ST state, (b) non-ST state.

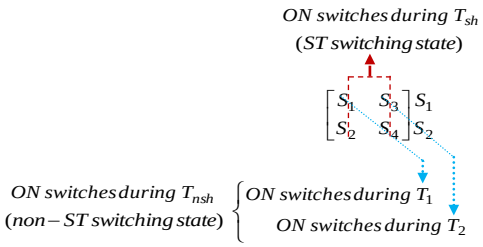

Fig. 3. First proposed control method.

where v_{L1} and v_{L2} are the voltages across the L_1 and L_2 inductors, V_{C1} and V_{C2} are the voltages across the C_1 and C_2 capacitors, and V_{dc} and v_o are the input and dc-link voltages of the inverter, respectively.

According to Fig. 2(b), in the non-ST switching state (T_{nsh} time interval), the diode of D is turned on, whereas, the switches have different states of turning on. In this mode, the following equations can be written:

$$v_{L1,nsh} = V_{dc} - V_{C1}\,,\quad v_{L2,nsh} = -V_{C2}\,,\quad v_{o,nsh} = V_{C1} + V_{C2} \qquad (2)$$

In steady-state, the average voltages across C_1 and C_2 capacitors (V_{C1} and V_{C2}) for all times can be calculated as follows [10], [19]:

$$V_{C1} = \frac{1-D_{sh}}{1-2D_{sh}}V_{dc}\,,\qquad V_{C2} = \frac{D_{sh}}{1-2D_{sh}}V_{dc} \qquad (3)$$

where D_{sh} is the duty cycle of the ST switching state, which can be defined as follows:

$$D_{sh} = \frac{T_{sh}}{T_s} = 1 - M \qquad (4)$$

where M is the modulation index of the inverter.

From Equs. (2) and (3), the maximum voltage across the dc-link ($v_{o,\max}$) is equal to [10], [19]:

$$v_{o,\max} = BV_{dc} = \frac{1}{1-2D_{sh}}V_{dc} \qquad (5)$$

where B is the boost factor of the qZSI.

By substituting Equ. (4) into Equ. (5), we have:

$$M = \frac{1}{2}\left(1 + \frac{V_{dc}}{v_{o,\max}}\right) \qquad (6)$$

Assuming a purely resistive load (R_L), the average current through the dc-link ($I_{o,av}$) for all times is equal to:

$$I_{o,av} = \frac{1-D_{sh}}{R_L}V_{o,\max} \qquad (7)$$

III. Proposed Mathematical PWM Control Methods for Single-Phase ZSIs

The various PWM strategies have been introduced to control the Z-source topologies [12]-[18]. The PWM strategies presented in [1] and [2] are based on mathematical equations. But, these PWM control methods have been designed for the inverter topologies based on voltage-source. Hence, in the inverter topologies based on the Z-source network, the ST switching state should be added to these control methods. In this paper, by using the concepts of PWM control methods presented in [1] and [2], three new PWM control methods based on mathematical equations are proposed for various single-phase Z-source topologies. The main purpose of these methods is to control the ST duty cycle (D_{sh}) through which a load can be able to see a controllable average voltage. In the mathematical proposed control methods, the sampling time (T_s) is divided into two time intervals as T_{sh} and T_{nsh} for the Z-source inverters, which can be written as follows:

$$T_s = T_{sh} + T_{nsh} \qquad (8)$$

where T_{sh} and T_{nsh} are the ST and non-ST switching states, respectively, which considering Equ. (6) can be obtained as follows:

$$T_{sh} = D_{sh}T_s = (1-M)T_s = \frac{T_s}{2}\left(1 - \frac{v_{dc}(t)}{v_{o,\max}(t)}\right) \qquad (9)$$

$$T_{nsh} = (1-D_{sh})T_s = MT_s = \frac{T_s}{2}\left(1 + \frac{v_{dc}(t)}{v_{o,\max}(t)}\right) \qquad (10)$$

Considering Equs. (8) and (10), the non-ST switching state (time interval of T_{nsh}) is also divided into two-time intervals such as T_1 and T_2 , which can be written as follows:

$$T_{nsh} = T_1 + T_2\ ;\ D_{sh}T_s \le T_i \le (1-D_{sh})T\ \ for\ i = 1,2 \qquad (11)$$

It is noticeable that the proposed strategy is based on a matrix of the switches (S), which can be defined as follows:

$$S = \begin{bmatrix} S_1 & S_3 \\ S_2 & S_4 \end{bmatrix}_{2\times 2} \qquad (12)$$

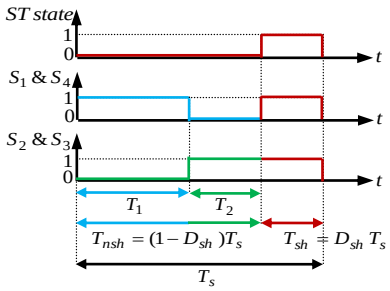

Fig. 4. Control signals of the first proposed PWM control method.

A. *First Proposed Control Method*

In the first proposed control method, the sequence of turning on and off for the switches is shown in Fig. 3. In the non-ST switching state (time interval of T_{nsh}), when the switches of S_1 and S_4 are turned on for the time interval of T_1, the switches of S_2 and S_3 should be turned off for this time and vice versa for the time interval of T_2. To generates the ST switching state (time interval of T_{sh}), the S_1 to S_4 switches are turned on. When the switching frequency of inverter (f_s) in comparison with the output frequency of inverter (f_L) has been selected big enough ($f_s >> f_L$), the average voltage across the output load (v_{Load}) can be obtained as follows [1]:

$$v_{Load}(t) = \frac{1}{T_{nsh}}(T_1 - T_2)v_{o,nsh} = \frac{1}{T_{nsh}}(T_1 - T_2)v_{o,\max}(t) \qquad (13)$$

From Equs. (11) and (13), the values of T_1 and T_2 are equal to:

$$T_1 = \frac{T_{nsh}}{2}\left(1 + \frac{v_{Load}(t)}{v_{o,\max}(t)}\right) \quad for \quad T_{sh} \le T_1 \le T_{nsh} \qquad (14)$$

$$T_2 = \frac{T_{nsh}}{2}\left(1 - \frac{v_{Load}(t)}{v_{o,\max}(t)}\right) \quad for \quad T_{sh} \le T_2 \le T_{nsh} \qquad (15)$$

Fig. 4 shows the first proposed control signals for the switches of single-phase inverter based on the Z-source network. The first control method can be analyzed under two conditions as follows:

1) Achieved Results for Constant Input and Balanced Output Voltage (CIBOV): In this case, the dc input voltage has the constant value, smooth and without the ripple, which can be defined as follows:

$$v_{dc}(t) = V_{dc} \qquad (16)$$

In the CIBOV case, the voltage of output load (v_{Load}) is considered as follows:

$$v_{Load}(t) = V_{o,\max}\sin\omega_L t \qquad (17)$$

where $V_{o,\max}$ and ω_L are the maximum and angular speed of the output load voltage, respectively.

By substituting Equs. (16) and (17) into Equs. (14) and (15), the values of T_1 and T_2 are equal to:

$$T_1 = \frac{(1 - D_{sh})T_s}{2}(1 + \sin\omega_L t) = \frac{M}{2f_s}(1 + \sin\omega_L t) \qquad (18)$$

$$T_2 = \frac{(1 - D_{sh})T_s}{2}(1 - \sin\omega_L t) = \frac{M}{2f_s}(1 - \sin\omega_L t) \qquad (19)$$

In this case, the current through the RL output load (i_{Load}) is equal to:

$$i_{Load}(t) = I_{o,\max}\sin(\omega_L t + \phi_L) \qquad (20)$$

where $I_{o,\max}$ is the maximum current through the RL output load and ϕ_L is the phase difference between the voltage and current of RL output load, which can be calculated as follows:

$$I_{o,\max} = \frac{V_{o,\max}}{\sqrt{R_L^2 + (L_L\omega_L)^2}} \quad , \quad \phi_{Load} = \tan^{-1}\left(\frac{L_L\omega_L}{R_L}\right) \qquad (21)$$

From Equ. (13), the relation between dc-link and output currents for the time interval of T_{nsh} can be calculated as follows [1]:

$$i_{o,nsh}(t) = \frac{1}{T_{nsh}}(T_1 - T_2)\,i_{Load}(t) \qquad (22)$$

Considering Equs. (18) to (22), in the non-ST switching state, the instantaneous current of dc-link ($i_{o,nsh}(t)$) is equal to:

$$i_{o,nsh}(t) = \frac{I_{o,\max}}{2}[\cos\phi_L - \cos(2\omega_L t + \phi_L)] \qquad (23)$$

2) Achieved Results for Ripple Input and Balanced Output Voltage (RIBOV): In this case, the dc input voltage has variable value, not smooth and with ripple, which can be defined as follows:

$$v_{dc}(t) = V_{dc} + V_r\sin\omega_r t \qquad \forall t: \; v_{dc}(t) > 0 \qquad (24)$$

By substituting Equ. (24) into Equs. (14) and (15), the values of T_1 and T_2 are equal to:

$$T_1 = \frac{(1 - D_{sh})T_s}{2}\left(1 + \frac{V_{o,\max}\sin\omega_L t}{V_{o,\max} + V_r\sin\omega_r t}\right) = \frac{M}{2f_s}\left(1 + \frac{V_{o,\max}\sin\omega_L t}{V_{o,\max} + V_r\sin\omega_r t}\right) \qquad (25)$$

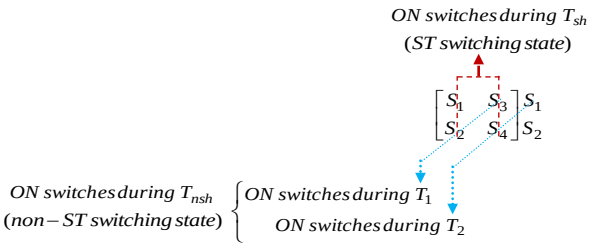

Fig. 5. Second proposed control method.

$$T_2 = \frac{(1-D_{sh})T_s}{2}\left(1-\frac{V_{o,\max}\sin\omega_L t}{V_{o,\max}+V_r\sin\omega_r t}\right) = \frac{M}{2f_s}\left(1-\frac{V_{o,\max}\sin\omega_L t}{V_{o,\max}+V_r\sin\omega_r t}\right) \quad (26)$$

B. Second Proposed Control Method

In the second proposed control method, the sequence of turning on and off for the switches is shown in Fig. 5. In this method for the time interval of T_{nsh}, the switches of S_2 and S_3 are turned on and the switches of S_1 and S_4 are turned off for the time interval of T_1, and vice versa for the time interval of T_2. The time interval of T_{sh} is similar to the first proposed method.

Considering $f_s >> f_L$, the average voltage across the output load (v_{Load}) is equal to:

$$v_{Load}(t) = \frac{1}{T_{nsh}}(-T_1+T_2)v_{o,nsh} = \frac{1}{T_{nsh}}(-T_1+T_2)v_{o,\max}(t) \quad (27)$$

From Equs. (11) And (27), the values of T_1 and T_2 are equal to:

$$T_1 = \frac{T_{nsh}}{2}\left(1-\frac{v_{Load}(t)}{v_{o,\max}(t)}\right) \quad for \quad T_{sh} \le T_1 \le T_{nsh} \quad (28)$$

$$T_2 = \frac{T_{nsh}}{2}\left(1+\frac{v_{Load}(t)}{v_{o,\max}(t)}\right) \quad for \quad T_{sh} \le T_2 \le T_{nsh} \quad (29)$$

The second proposed control signals for the switches of single-phase Z-source inverter are shown in Fig. 6. This control method can be analyzed under two conditions as follows:

1) Achieved Results for Constant Input and Balanced Output Voltage (CIBOV): In this case, by placing Equs. (16) And (17) into Equs. (28) And (29), the values of T_1 and T_2 are equal to:

$$T_1 = \frac{(1-D_{sh})T_s}{2}(1-\sin\omega_L t) = \frac{M}{2f_s}(1-\sin\omega_L t) \quad (30)$$

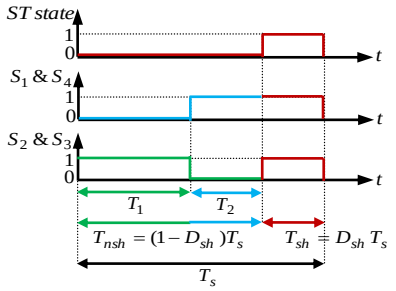

Fig. 6. Control signals of the second proposed PWM control method.

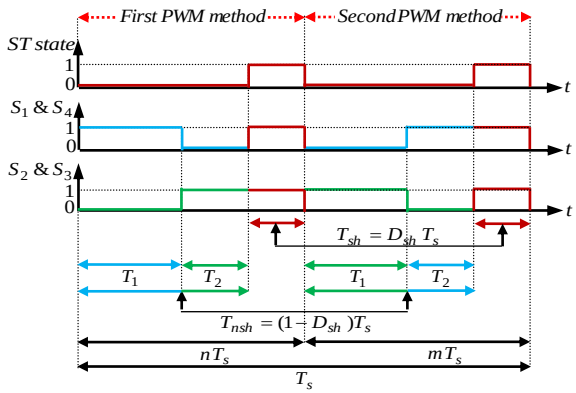

Fig. 7. Control signals of the third proposed PWM control method.

$$T_2 = \frac{(1-D_{sh})T_s}{2}(1+\sin\omega_L t) = \frac{M}{2f_s}(1+\sin\omega_L t) \quad (31)$$

2) Achieved Results for Ripple Input and Balanced Output Voltage (RIBOV): In this case, by placing Equs. (17) And (24) into Equs. (28) And (29), the values of T_1 and T_2 are equal to:

$$T_1 = \frac{(1-D_{sh})T_s}{2}\left(1-\frac{V_{o,\max}\sin\omega_L t}{V_{o,\max}+V_r\sin\omega_r t}\right) = \frac{M}{2f_s}\left(1-\frac{V_{o,\max}\sin\omega_L t}{V_{o,\max}+V_r\sin\omega_r t}\right) \quad (32)$$

$$T_2 = \frac{(1-D_{sh})T_s}{2}\left(1+\frac{V_{o,\max}\sin\omega_L t}{V_{o,\max}+V_r\sin\omega_r t}\right) = \frac{M}{2f_s}\left(1+\frac{V_{o,\max}\sin\omega_L t}{V_{o,\max}+V_r\sin\omega_r t}\right) \quad (33)$$

C. Third Proposed Control Method

By combining both the first and second proposed PWM methods, the third control method is proposed. In this method, a sampling time period is divided into two sections such as n and m, which are shown in Fig. 7. The third proposed

control signals for the switches of single-phase Z-source inverter are shown in Fig. 7.

According to Equs. (13) And (27), the average voltage across the output load (v_{Load}) can be obtained as follows:

$$v_{Load}(t)=\left[\frac{n}{T_{nsh}}(T_1-T_2)+\frac{m}{T_{nsh}}(-T_1+T_2)\right]v_{o,\max}(t) \qquad (34)$$

IV. Comparison

Various PWM control methods have been introduced for the ZSI topologies. But overall they can be classified into carrier-based PWM strategies [12]-[18]. In this technique, the control signals for switch gates generate from the comparison of linear or curve reference waves with the triangular carrier waveform. Hence, the pulse widths of signal gates can be equal or unequal which causes the values of the ST duty cycle will respectively be constant or variable [9], [12].

Three fundamental and most important PWM control methods are related to the simple boost control (SBC), maximum boost control (MBC), and maximum constant boost control (MCBC) [9], [12]. Table I and Figs. 8 and 9 present a comparison between the three techniques of SBC, MBC, and MCBC. Considering Table I and Figs. 8 and 9, the SBC method is used to control of D_{sh} (ST duty cycle) in which the ST time per switching cycle is kept constant. Hence, the boost factor will be a constant value. Under these conditions, the dc inductor current and capacitor voltage, which are associated with the output frequency, will have no ripples. In this strategy, the value of D_{sh} is decreased with the increase of M, which causes relatively high voltage stress across the devices. In the MBC method, the ST time per switching cycle is variable. MBC in comparison with SBC not only reduces the voltage stress across the devices for the same modulation index but also increases the voltage boost factor and inverter voltage gain. However, it has the drawbacks of low-frequency ripples on the Z-source network. So that the inductor current ripple becomes significant when the output frequency is low, and a large inductor is required. In order to reduce the volume and cost of the LC network, the elimination of low-frequency current ripple is needed by using a constant ST duty cycle. At the same time, a higher voltage boost and lower voltage stress for any given modulation index are simultaneously demanded. The MCBC method is introduced to achieve the above aims [9], [12].

Proposed control methods not only can be achieved all the benefits of SBC, MBC, and MCBC but also they have a number of unique advantages that are listed below:

- The most important advantage of the proposed control methods is having a mathematical basis.

TABLE I
Comparison of SBC, MBC, and MCBC Strategies.

PWM method	ST duty cycle	Voltage boost factor	Inverter voltage gain	Devices voltage stress
	$D_{sh}=\frac{T_{sh}}{T}$	$B=\frac{1}{1-2D_{sh}}$	$G=M\times B$	V_s/V_{dc} versus G
SBC	$1-M$	$\frac{1}{2M-1}$	$\frac{M}{2M-1}$	$2G-1$
MBC	$\frac{2\pi-3\sqrt{3}M}{2\pi}$	$\frac{\pi}{3\sqrt{3}M-\pi}$	$\frac{\pi M}{3\sqrt{3}M-\pi}$	$\frac{3\sqrt{3}G-M}{\pi}$
MCBC	$1-\frac{\sqrt{3}M}{2}$	$\frac{1}{\sqrt{3}M-1}$	$\frac{M}{\sqrt{3}M-1}$	$\sqrt{3}G-1$

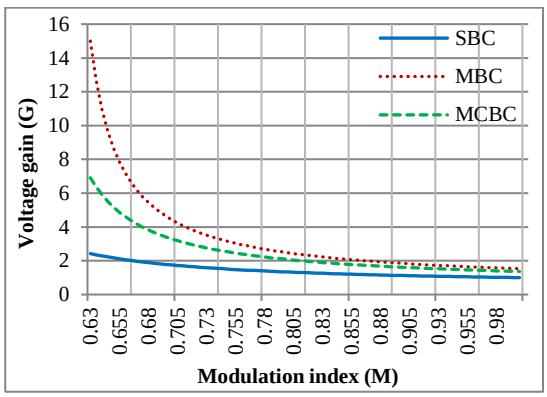

Fig. 8. Comparison of voltage gain versus modulation index.

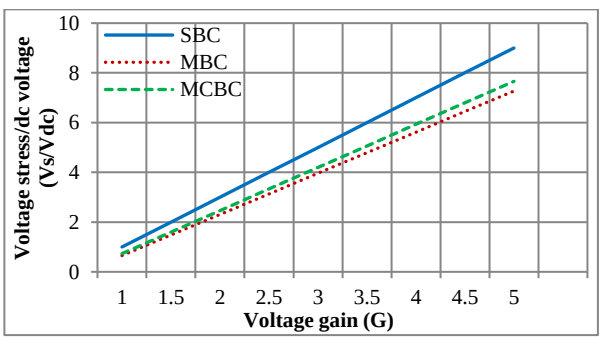

Fig. 9. Comparison of normalized devices voltage stress versus voltage gain.

- Considering Equs. (4) to (6), the used relationship between D_{sh} and M is related to the SBC method. Hence, all obtained results for the proposed methods will be under this technique. However, due to the capability of the proposed methods, the D_{sh} and M relationship related to the MBC or MCBC methods can be used instead of the SBC.
- The switching states of the SBC, MBC, and MCBC are generated by comparing two straight lines or two curves with a triangle carrier waveform each of which had its own advantages and disadvantages. But the proposed control methods have used a series of mathematical

equations for generating the switching states which can overcome their disadvantages (such as higher harmonics and THD).

- According to Fig. 7 ($nT_s + mT_s = T_s$ or $n+m=1$), the n or m can be used to control the one parameter of the inverter. Thus, in the third proposed technique, not only the voltage and current can be controlled but also it can control (or eliminate) the extra parameters such as harmonic and THD without any hardware elements.

V. Simulation Results and Discussion

In this paper, the proposed PWM methods are implemented for qZSI topology. To prove the correct performance of the proposed PWM control methods under CIBOV and RIBOV conditions, the achieved results of the simulation are used. Moreover, in the same condition, a comparison is done between proposed and SBC methods in terms of harmonics, THD, and dynamic response. Table II shows the used parameters for the simulations.

A. *Check the Correct Operation of the Proposed Control Methods*

Figs. 10 to 15 show the simulation results of the proposed PWM control methods for single-phase qZSI under CIBOV and RIBOV operations. According to Table II, the input voltage source and the maximum amplitude of RL output load voltage are equal to $V_{dc} = 50V$ and $V_{o,\max} = 250V$, respectively. That means the boost factor of the inverter is equal to $B = 5$. Simulation Results for Single-Phase qZSI under three proposed control methods can be analyzed as follows:

1) Obtained Results for the First Control Method: Figs. 10 and 11 show the simulation results for the first proposed PWM control method under CIBOV and RIBOV operations, respectively. From Equs. (6) and (4), the modulation index and duty cycle should be $M = 0.6$ and $D_{sh} = 0.4$, respectively. From Equs. (1) and (2), the obtained voltages across the dc-link of qZSI for ST and non-ST states are $v_{o,sh} = 0V$ and $v_{o,nsh} = 250V$, respectively, which are shown in Figs. 10(b) and 11(a). The voltage and current of RL output load under CIBOV and RIBOV operations are shown in Figs. 10(d, e) and 11(c, d), respectively.

2) Obtained Results for the Second Control Method: Figs. 12 and 13 show the simulation results for the second proposed PWM control method under CIBOV and RIBOV operations, respectively. From Equs. (1) and (2), the obtained voltages across the dc-link of qZSI for ST and non-ST states should be $v_{o,sh} = 0V$ and $v_{o,nsh} = 250V$, respectively, which are shown in Figs. 12(b) and 13(a). The voltage and current of RL output load under CIBOV and RIBOV operations are shown in Figs. 12(d, e) and 13(c, d), respectively.

3) Obtained Results for the Third Control Method: Figs. 14 and 15 show the simulation results for the third proposed PWM control method under CIBOV and RIBOV operations, respectively. Figs. 14(b) and 15(a) show the obtained voltages across the dc-link for ST and non-ST states, respectively. Figs. 14(d, e) and 15(c, d) show the voltage and current of RL output load under CIBOV and RIBOV operations, respectively.

As a result, considering the obtained theoretical and simulation results, the simulation results shown in Figs. 10 to 15 are similar to the theoretical analysis, which proves the suitable performance of the proposed PWM control methods.

TABLE II
USED PARAMETERS FOR THE SIMULATION.

Quantity	Symbol	Value
Input voltage source	V_{dc}	$50V$
Maximum output voltage	$V_{o,\max}$	$250V$
Z-source network	$C_1 = C_2$	$2mF$
	$L_1 = L_2$	$0.5mH$
Output load values	R_L	40Ω
	L_L	$5mH$
	f_L	$50Hz$
Switching frequency	f_s	$20kHz$

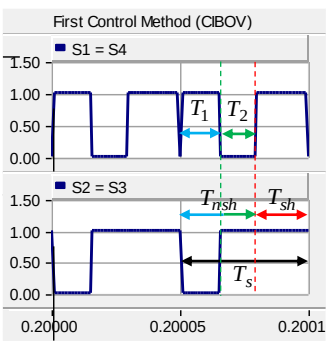

(a)

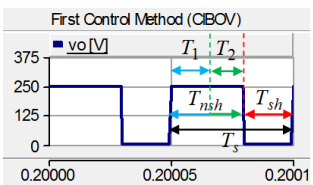

(b)

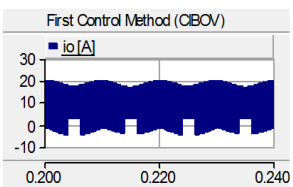

(c)

Fig. 10. continued

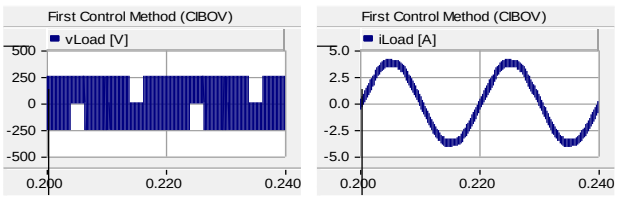

(d) (e)

Fig. 10. Simulation results for the first proposed PWM control method under CIBOV operation; (a) gate pulses of switches, (b) voltage of dc-link, (c) current of dc-link, (d) voltage of RL output load, (e) current of RL output load.

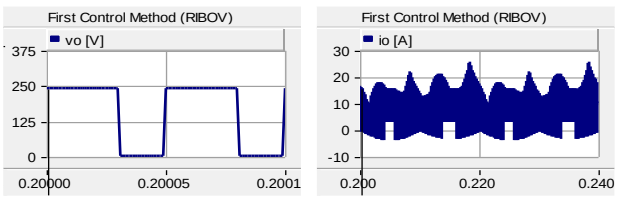

(a) (b)

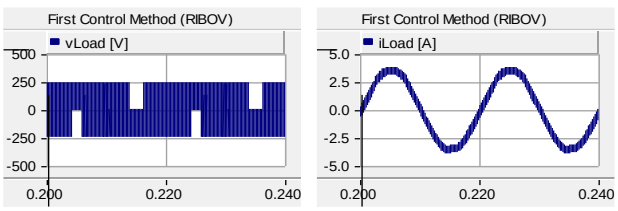

(c) (d)

Fig. 11. Simulation results for the first proposed PWM control method under RIBOV operation; (a) dc-link voltage, (b) current of dc-link, (c) voltage of RL output load, (d) current of RL output load.

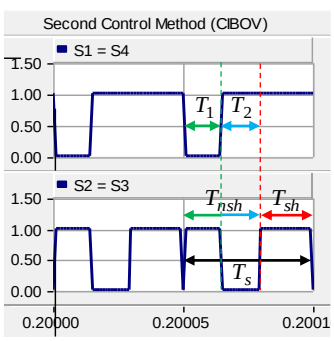

(a)

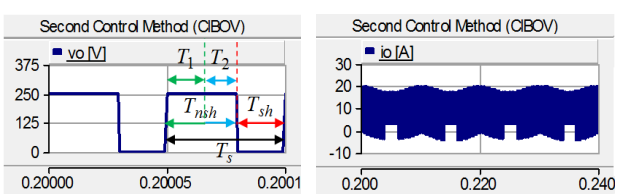

(b) (c)

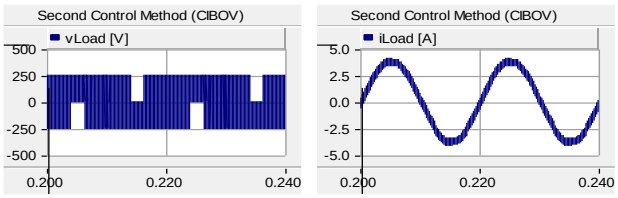

(d) (e)

Fig. 12. Simulation results for the second proposed PWM control method under CIBOV operation; (a) gate pulses of switches, (b) voltage of dc-link, (c) current of dc-link, (d) voltage of RL output load, (e) current of RL output load.

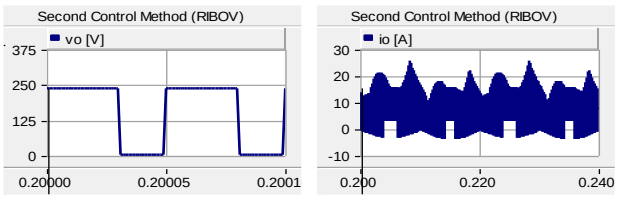

(a) (b)

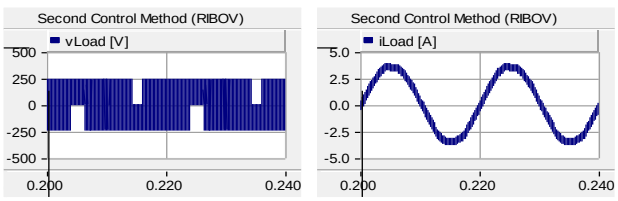

(c) (d)

Fig. 13. Simulation results for the second proposed PWM control method under RIBOV operation; (a) dc-link voltage, (b) current of dc-link, (c) voltage of RL output load, (d) current of RL output load.

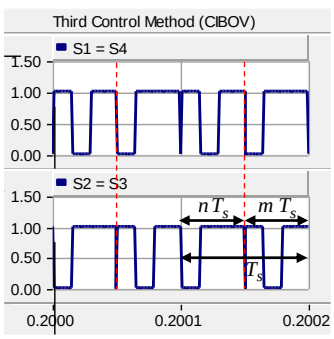

(a)

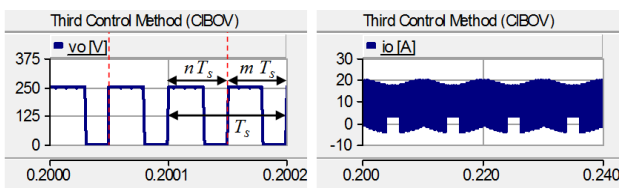

(b) (c)

Fig. 14. continued

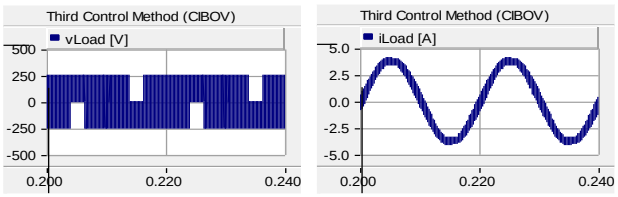

(d) (e)

Fig. 14. Simulation results for the third proposed PWM control method under CIBOV operation; (a) gate pulses of switches, (b) voltage of dc-link, (c) current of dc-link, (d) voltage of *RL* output load, (e) current of *RL* output load.

B. Harmonic and THD Analysis

The harmonic spectrums and THD results of output voltage and current for the proposed and SBC control methods under different operational conditions are illustrated in Figs. 16 to 19. In CIBOV and RIBOV cases, the harmonics components of the proposed methods are less than the SBC method (Figs. 16 and 18). Also, the THD of the output voltage for the proposed methods is less than the SBC method (Figs. 17 and 19). The THD of the output current for the first and second proposed methods is almost equal to the SBC method. But, it has a lower value for the third proposed method. In addition, the reduction of harmonics and THD values for the third proposed strategy is more in comparison with the first and second proposed methods (Figs. 17 and 19).

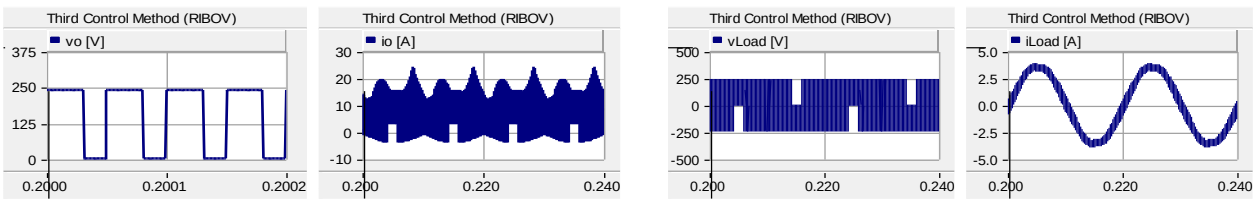

(a) (b) (c) (d)

Fig. 15. Simulation results for the third proposed PWM control method under RIBOV operation; (a) dc-link voltage, (b) current of dc-link, (c) voltage of *RL* output load, (d) current of *RL* output load.

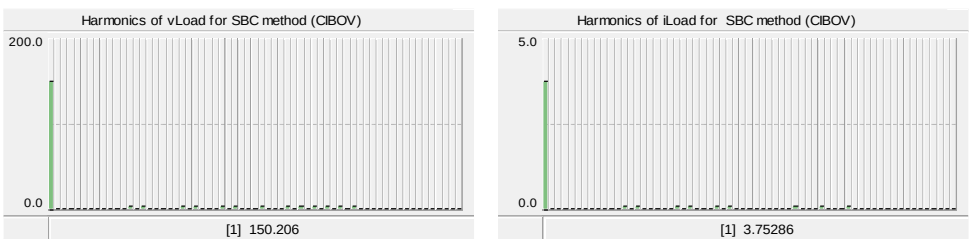

(a)

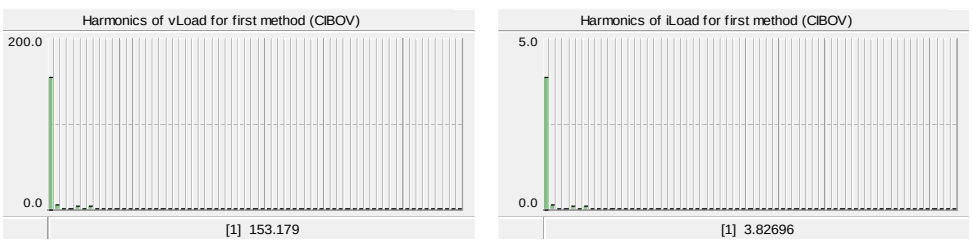

(b)

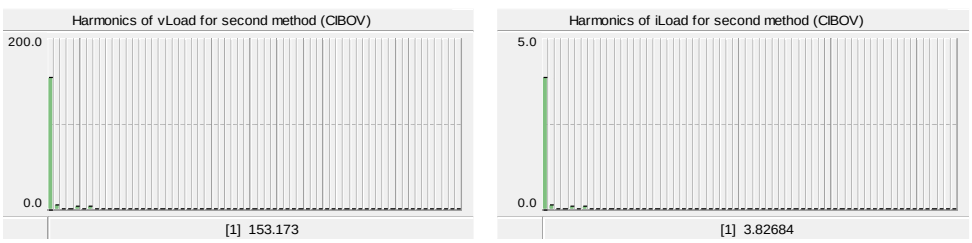

(c)

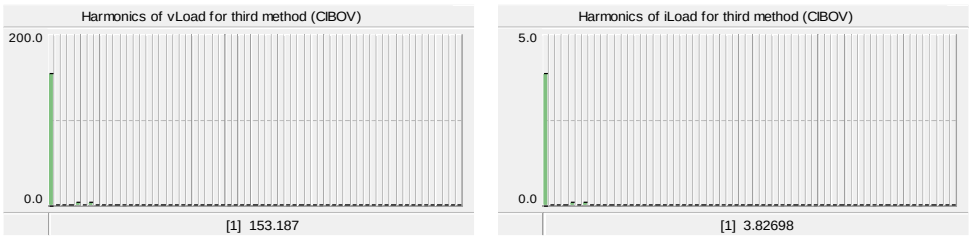

(d)

Fig. 16. Harmonic spectrums under CIBOV operation; (a) SBC method, (b) first proposed method, (c) second proposed method, (d) third proposed method.

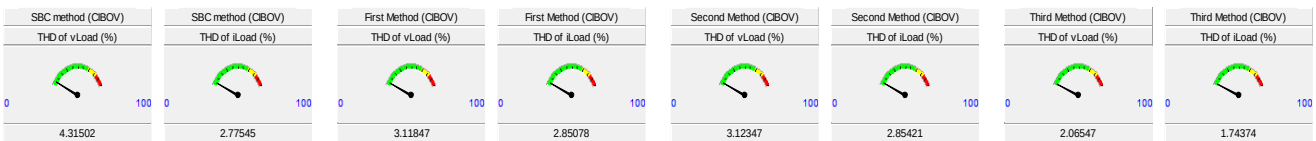

(a) (b) (c) (d)

Fig. 17. THD analysis under CIBOV operation; (a) SBC method, (b) first proposed method, (c) second proposed method, (d) third proposed method.

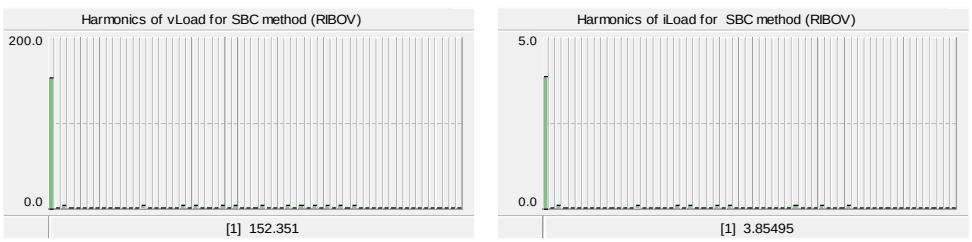

(a)

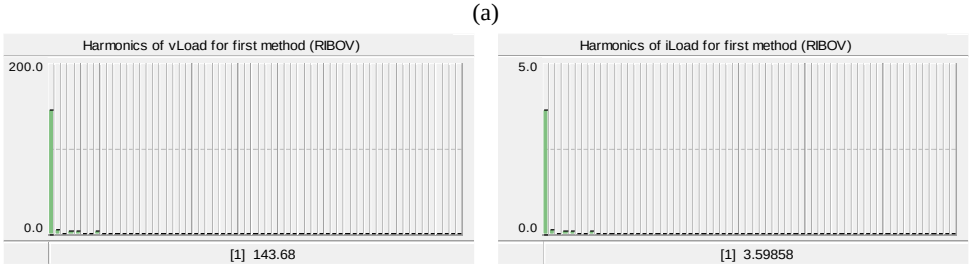

(b)

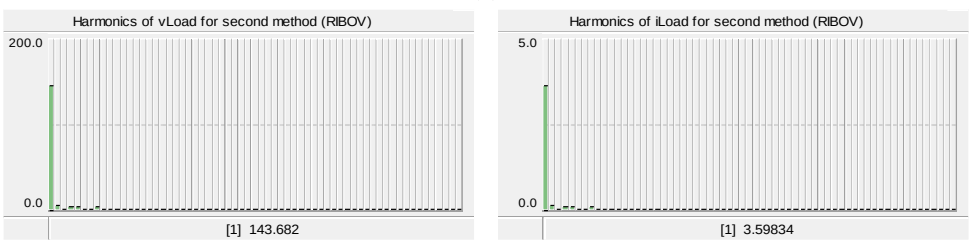

(c)

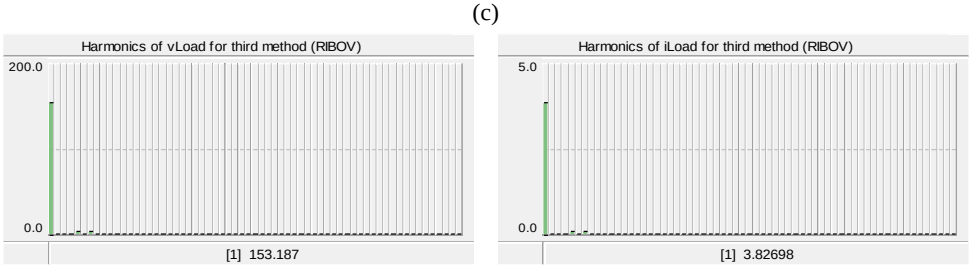

(d)

Fig. 18. Harmonic spectrums under RIBOV operation; (a) SBC method, (b) first proposed method, (c) second proposed method, (d) third proposed method.

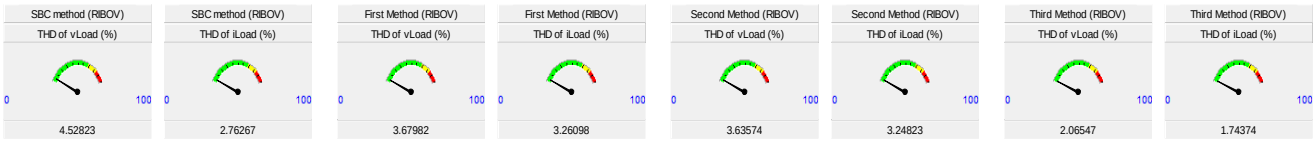

(a) (b) (c) (d)

Fig. 19. THD analysis under RIBOV operation; (a) SBC method, (b) first proposed method, (c) second proposed method, (d) third proposed method.

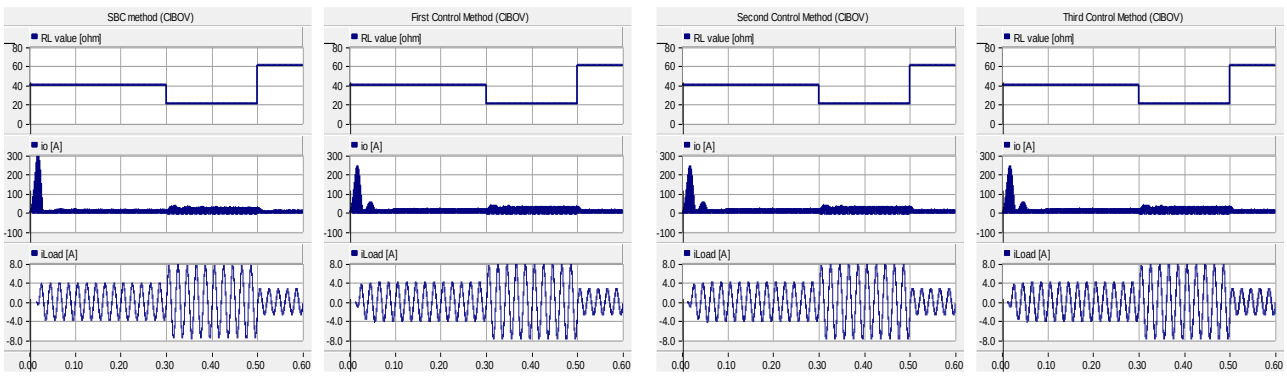

(a) (b) (c) (d)

Fig. 20. Dynamic response evaluation under CIBOV operation; (a) SBC method, (b) first proposed method, (c) second proposed method, (d) third proposed method.

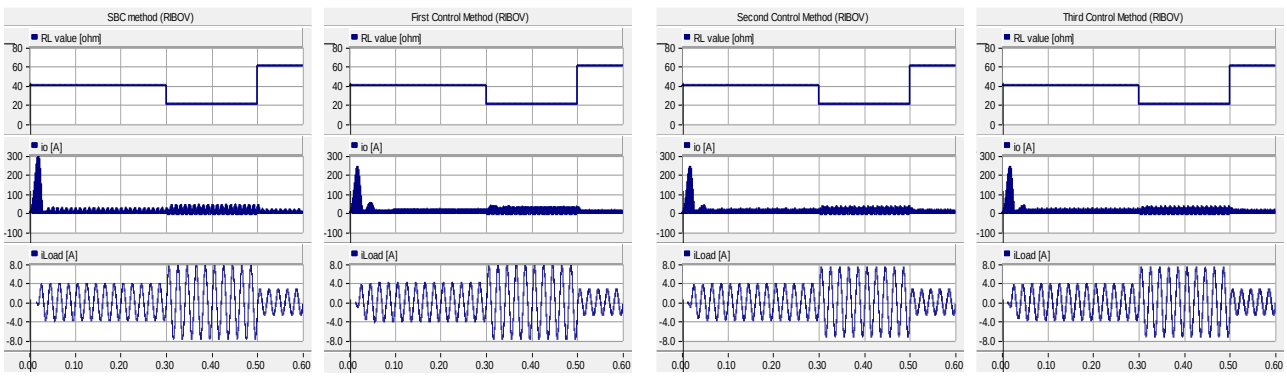

(a) (b) (c) (d)

Fig. 21. Dynamic response evaluation under RIBOV operation; (a) SBC method, (b) first proposed method, (c) second proposed method, (d) third proposed method.

C. Dynamic Response Evaluation

In order to dynamic change evaluation in the output of qZSI, the output resistance value (R_L) will be changed among 20, 40, and 60 ohms. During this evaluation, the output inductor value has a constant value ($L_L = 5\,mH$). Figs. 20 and 21 show dynamic change evaluation in the qZSI output by using the proposed and SBC control techniques under CIBOV and RIBOV operations. For different values of output resistance (R_L), the simulation results shown in Figs. 20 and 21 demonstrate the appropriate operating of dynamic changes in the qZSI output for proposed methods under CIBOV and RIBOV operations. Also, the output current in the proposed strategies has a lower amplitude in the transient mode in comparison with the SBC method.

VI. CONCLUSION

The design of a suitable control method for the inverters can be an effective solution to the elimination of low order harmonics, the lower value for THD, and decreasing the size and cost of the filter. Hence, in this paper, three new PWM control methods based on mathematical equations were proposed for controlling the various single-phase ZSIs. The proposed methods can also be extended to the various three-phase Z-source topologies. Regardless of whether the input voltage is constant or variable, the proposed PWM techniques can produce a desired balanced and unbalanced

voltage at the output of the inverter. The proposed methods were analyzed under different circumstances (CIBOV and RIBOV), which the worthiness of them was confirmed by obtained simulation results in PSCAD software.

REFERENCES

[1] E. Babaei, "A new pulse with modulation technique for inverters," *Arabian Journal for Science and Engineering*, Vol. 39, No. 8, pp. 6235-6247, Aug. 2014.

[2] E. Babaei and M. Sabahi, "Development of pulse with modulation technique for controlling invrters under balanced and unbalanced operations," *Arabian Journal for Science and Engineering*, Vol. 39, No. 4, pp. 2941-2951, Apr. 2013.

[3] S. Xiao, T. Shi, X. Li, Z. Wang, and C. Xia, "Single-current-sensor control for PMSM driven by quasi-Z-source inverter," *IEEE Trans. Power Electron.*, Vol. 34, No.7, pp. 7013-7024, Jul. 2019.

[4] N. Vosoughi, S. H. Hosseini, and Mehran Sabahi, "A new transformer-less five-level grid-tied inverter for photovoltaic applications," *IEEE Trans. Energy Convers.*, Vol. 35, No.1, pp. 106-118, Mar. 2020.

[5] X. Guo, N. Wang, J. Zhang, B. Wang, and M.K. Nguyen, "A novel transformerless current source inverter for leakage current reduction," IEEE Access, Vol. 7, pp. 50681-50690, Apr. 2019.

[6] T. Ahmadzadeh, E. Babaei, M. Sabahi, and T. Abedinzadeh, "An improved transformerless grid-connected PV system with related control strategy to reduce leakage current, extract maximum power point and control power," *Iranian Journal of Electrical and Electronic Engineering (IJEEE)*, Vol. 16, No.4, pp. 513-523, Dec. 2020.

[7] A. Karbalaei and M. Mardaneh, "Improved symmetric switched-inductor/capacitor quasi Z-source inverter with ability uplifted-boost," *International Journal of Industrial Electronics, Control and Optimization (IECO)*, Vol. 3, No. 1, pp. 47-58, Jan. 2020.

[8] A. Karbalaei and M. Mardaneh, "Improved symmetric switched-inductor/capacitor quasi Z-source inverter with ability uplifted-boost," *International Journal of Industrial Electronics, Control and Optimization (IECO)*, Vol. 3, No. 1, pp. 47-58, Jan. 2020.

[9] E. Babaei and T. Ahmadzadeh, "A new structure of buck-boost Z-source converter based on Z-H converter," *Journal of Operation and Automation in Power Engineering (JOAPE)*, Vol. 4, No. 2, pp. 25-39, Dec. 2016.

[10] T. Ahmadzadeh and E. Babaei, "Improved quasi-Z-source based three-Phase three-Level neutral point clamped inverter," in *Proc. PEDSTC*, pp. 99-103, 2018.

[11] T. Ahmadzadeh, E. Babaei, and M. Sabahi, "Modified PWM control method for neutral point clamped ultilevel inverters," in *Proc. ECTICON*, pp. 765-768, 2017.

[12] M. Shen, J. wang, A. Joseph, F. Z. peng, L. M. Tolbert, and D. J. Adams "Constant Boost Control of the Z-Source Inverter to Minimize Current Ripple and Voltage Stress," *IEEE Trans. Ind. Appl.*, Vol. 42, No.3, pp. 770-778, May/Jun. 2006.

[13] R. Iijima, T. Isobe, and H. Tadano, "Optimized short-through time distribution for inductor current ripple reduction in Z-source inverters using space-vector modulation," *IEEE Trans. Ind. Appl.*, Vol. 55, No. 3, pp. 2922-2930, May/Jun. 2019.

[14] S. Singh and S. Sonar , "A new SVPWM technique to reduce the inductor current ripple of three-phase Z-source inverter," *IEEE Trans. Ind. Electron.*, Vol. 67, No. 5, pp. 3540-3550, May. 2020.

[15] D. Shuai and Z. Qianfa, "Analysis and control of current ripples of Z-source inverters," *IEEE Access*, Vol. 8, pp. 41220-41228, Feb. 2020.

[16] M. Mohammadi, J.S. Moghani, and J. Milimonfared, "A novel dual switching frequency modulation for Z-source and quasi-Z-source inverters," *IEEE Trans. Ind. Electron.*, Vol. 65, No. 6, pp. 5167-5176, Jun. 2018.

[17] W. Xu, M. Liu, J. Liu, K.W. Chan, and K.W.E. Cheng, "A series of new control methods for single-phase Z-source inverters and the optimized operation," *IEEE Access*, Vol. 7, pp. 113786-113800, Aug. 2019.

[18] L. Hang, U. Subramaniam, G. Bayrak, H. Moayedi, D. Ghaderi, and M.R. Minaz, "Influence of a proposed switching method on reliability and total harmonic distortion of the quasi Z-source inverters," *IEEE Access*, Vol. 8, pp. 33088-33100, Feb. 2020.

[19] M. K. Nguyen, Y. C. Lim, and S. J. Park, "A comparison between single-phase quasi-Z-source and quasi-switched boost inverters," *IEEE Trans. Ind. Electron.*, Vol. 62, No. 10, pp. 6336-6344, Oct. 2015.

Taher Ahmadzadeh was born in Tabriz, Iran in 1986. He received his A.Sc. degree in Electronic Engineering from Islamic Azad University, Ahar Branch, Ahar, Iran, in 2006, his B.Sc. degree in Electronic Engineering from Islamic Azad University, Tabriz Branch, Tabriz, Iran, in 2009, and his M.Sc. degree in Electrical Engineering from the Aras International Campus, University of Tabriz, Tabriz, Iran, in 2014. He is currently working towards his Ph.D. degree in Electrical Engineering from the Department of Engineering, Shabestar Branch, Islamic Azad University, Shabestar, Iran. His current research interests include the analysis and control of power electronic converters and their applications.

Ebrahim Babaei was born in Ahar, Iran, in 1970. He received his B.Sc. degree in Electronic Engineering and his M.Sc. degree in Electrical Engineering from the Department of Engineering, University of Tabriz, Tabriz, Iran, in 1992 and 2001, respectively, graduating with first-class honors. He received his Ph.D. degree in Electrical Engineering from the Department of Electrical and Computer Engineering, University of Tabriz, in 2007. In 2004, he joined the Faculty of Electrical and Computer Engineering, University of Tabriz. He was an assistant professor from 2007 to 2011, an associate professor from 2011 to 2015 and has been a professor since 2015. He is the author of more than 300 journal and conference papers. He also holds 17 patents in the area of power electronics. His current research interests include the analysis and control of power electronic converters and their applications, dynamic power system, power system transients. Prof. Babaei has been the Editor-in-Chief of the Journal of Electrical Engineering of the University of Tabriz, since 2013. He is also currently an Associate Editor of the IEEE TRANSACTIONS ON

INDUSTRIAL ELECTRONICS. He is a Guest Editor for a special issue on “Recent Advances in Multilevel Inverters and their Applications” in the IEEE Transactions on Industrial Electronics. In 2013, he was the recipient of the Best Researcher Award from the University of Tabriz. Prof. Babaei has been included in the Top One Percent of the World’s Scientists and Academics according to Thomson Reuters' list in 2015.

Mehran Sabahi was born in Tabriz, Iran, in 1968. He received his B.Sc. degree in Electronic Engineering from the University of Tabriz, his M.Sc. degree in Electrical Engineering from Tehran University, Tehran, Iran, and his Ph.D. degree in Electrical Engineering from the University of Tabriz, in 1991, 1994, and 2009, respectively. In 2009, he joined the faculty of electrical and computer engineering at the University of Tabriz where he has been an associate professor since 2015. His current research interests include power electronic converters and renewable energy systems.

Taher Abedinzadeh was born in Khoy, Iran, in 1983. He received his B.Sc. degree in Electrical Engineering from Iran University of Science and Technology, Tehran, Iran, in 2005, his M.Sc. degree in Electrical Engineering from the Sharif University of Technology, Tehran, Iran, in 2007, and his Ph.D. degree in Electrical Engineering from Islamic Azad University, Science and Research Branch, Tehran, Iran, in 2014. He is a Faculty Member of Islamic Azad University-Shabestar Branch, Shabestar, Iran. His current research interests include power systems, smart grids, and renewable energies.

IECO

This page intentionally left blank.